Dynamics of strong-field photoionization in two dimensions for short-range binding potentials

Jacek Matulewski,* Andrzej Raczyński, and Jarosław Zaremba
Instytut Fizyki, Uniwersytet Mikołaja Kopernika, ulicka Grudziądzka 5, 87-100 Toruń, Poland
(Received 27 February 2003; published 18 July 2003)

Photodetachment in an ultrastrong laser field in two spatial dimensions is investigated *ab initio*. A qualitative behavior of the packet for a short-range binding potential is contrasted with that for a soft-core potential, in particular, dynamical effects due to a rescattering of fragments separated from the main packet are demonstrated.

DOI: 10.1103/PhysRevA.68.013408 PACS number(s): 42.50.Hz, 32.80.Rm, 32.80.Gc

I. INTRODUCTION

The problem of ultrastrong-field photoionization has been the subject of studies in quantum optics for the last fifteen years (for a recent review see Ref. [1]). Because of enormous technical difficulties most of *ab initio* calculations were performed for one-dimensional models. It is well known that if the electric-field amplitude ε_0 grows in the region of a few atomic units (for a typical frequency $\omega=1$ a.u. and a binding potential supporting an initial state of energy of the order of 1 a.u.), the ionization rate need not grow monotonically with the field and the population can be regarded as trapped in a Kramers-Henneberger (KH) well [2]. At a field amplitude of about 10 a.u. almost no probability leaks from the neighborhood of the nucleus. Unfortunately, one-dimensional models fail to represent important features of real systems; in particular, they can imitate only an interaction with a linearly polarized field in the dipole approximation. Thus, investigating magnetic interactions or light polarization effects requires a generalization to models with more spatial dimensions [3]. Investigations performed in two dimensions for long-range binding potentials predict, in particular, that the stabilization at field intensities higher than 10 a.u. is destroyed by a nondipole kinetic effect, the so-called magnetic drift of the packet as a whole away from the region of the nucleus.

The aim of this paper is to study photodetachment in superintense fields (such that the Schrödinger equation is still valid), in two dimensions, in the situation which has not yet been investigated in a few so far existing papers [3,5,6]; in comparison with other papers, the long-range atomic potential is replaced by a short-range potential well (radial and rectangular). The details of the dynamics in our case include some special effects, an interpretation of which is necessary for a complete understanding of the process.

A new element in comparison with earlier papers [3] is that the well potential (especially, if it has deep eigenstates), due to its steep edges, causes tearing of the oscillating wave packet into fragments, even in such strong laser field intensities as 15–20 a.u. Because of the wave-packet tearing, the classical model does not allow to satisfactorily interpret all numerical results. In particular, satellite wave-packet's fragments detached at different times and being of a significant size can be rescattered in their oscillatory motion and interfere, with the details of the process depending on the shape of the laser pulse, in particular, on the position of the classical packet's turning points. The phase dependence of the dynamics is also discussed.

II. THE BINDING POTENTIAL AND THE SHAPE OF THE PULSE

There are two types of model atomic potentials commonly used in the studies on the interaction of atomic systems with superstrong fields in one dimension: a soft-core Coulomb potential proposed by Su, Javanainen, and Eberly in a series of papers [4] and a short-range potential of a negative ion, modeled, e.g., by a rectangular well. The main difference is that the former potential is smooth and supports an infinite number of discrete states, while the latter one has two points of discontinuity and a few bound states. In the latter case, the packet has less chances to remain a connected structure (i.e., it is more exposed to tearing) and cannot be dynamically stabilized, i.e., trapped in the series of the Rydberg states.

While two-dimensional studies on the strong-field stabilization of models with a soft-core potential have already been reported (see Refs. [1,6]), in this paper, we concentrate on special effects due to a potential well, which we assume to be radial, i.e., we take

$$V(\vec{r}) = -V_0\,\theta(a-r), \tag{1}$$

where $r=\sqrt{x^2+y^2}$ and θ is the step function. The width $2a$ and the depth V_0 of the well are chosen so that there is only a single (initial) bound state.

The choice of the pulse shape is also very important for the dynamics of the ionization process. The stabilization is possible only if the pulse does not lead to a fast drift of the electron, i.e., the classical trajectory of the electron in the absence of the binding potential remains close to the nucleus. The results presented below are obtained for rectangular cosinusoidal pulses which satisfy this condition. For a pulse propagating along the y axis and with x polarization, we thus take the field amplitude $\vec{\varepsilon}(y,t)=\hat{x}\varepsilon_0\cos(ky-\omega t)$ or the vector potential $\vec{A}(y,t)=-\hat{x}(\varepsilon_0/\omega)\sin(ky-\omega t)$. The continuous pulses often adopted in other papers (e.g., those with trapezoid envelope) may imply complicated switch-on effects, especially if no dipole approximation is made. For example,

*Electronic address: jacek@phys.uni.torun.pl

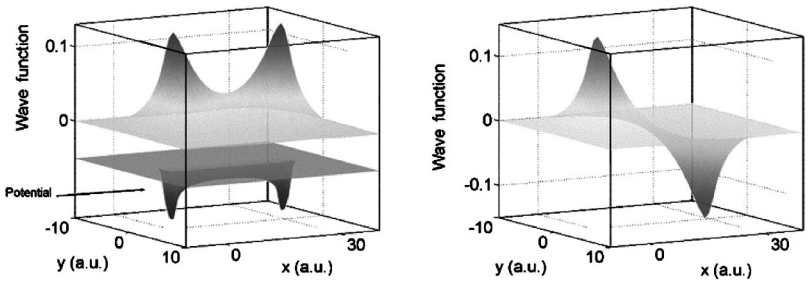

FIG. 1. The KH averaged potential for a quantum well potential ($a=1$ a.u., $V_0=2$ a.u.) and a cosine pulse ($\varepsilon_0=15$ a.u., $\omega=1$ a.u.). On the left, the KH potential and the ground-state wave function with energy $E_1=-0.0192$ a.u. On the right, the wave function of the only excited state ($E_2=-0.0158$ a.u.).

they may give rise to a field component which is not an electromagnetic wave. Moreover, calculating the vector potential by a time integral of the electric field introduces ambiguities reflecting various possible experimental realizations. We have checked that the effect we describe below appears also in a modified version for a trapezoid envelope.

The cosine pulse with any initial phase has an important feature in contradistinction to other pulses usually assumed in this context, namely, the turning points are shifted asymmetrically with respect to the potential well, with one of them located at the well, i.e., at the initial position of the wave packet. If $\varepsilon(t)=\varepsilon_0\cos(\omega t)$, the electron free of the binding potential would, in one dimension, oscillate in the range $(-2\varepsilon_0/\omega^2,0)$, which means that the right turning point occurs at the well.

Strong-field ionization is very often described in terms of the KH well. In Kramers frame an unbounded electron stays at rest and experiences the interaction of the oscillating nucleus. The KH potential well is just this interaction averaged over the oscillation period or, in other words, the zeroth term of the Fourier series of the interaction. In the initial stage of ionization, the electron's wave packet spreads out until it has reached the size of the KH well. Further changes of the packet's shape as well as its slow drift may be explained as due to higher terms of the Fourier expansion.

For the cosinusoidal pulse, the electron is initially located close to one of the two minima of the KH well, in contradistinction to the case of other pulses studied in this context, for which its initial position occurs in the middle.

In the present work, we will demonstrate how the results of the one-dimensional computations must be completed and developed in the case of two spatial dimensions. In particular, the Kramers frame and the corresponding KH well are now introduced as if there were no movement in the direction perpendicular to the electric field $\vec{\varepsilon}(\vec{r},t)=\hat{x}\varepsilon_0\cos(ky-\omega t)$: the transformation accounts for the electron movement $X(t)=(\varepsilon_0/\omega^2)[1-\cos(\omega t)]$, while its slow drift in the x direction and/or its throwing away of small parts in both directions are due to the higher terms of the Fourier expansion. The evolution in the y direction includes also magnetic effects seen as throwing away of small pieces rather than a drift of the packet as a whole. This aspect of the two-dimensional ionization process has not been observed in other works on strong-field ionization because they were dealing with soft-core binding potentials, in contradistinction to short-range potentials considered in this paper.

The KH well has the form

$$V_{KH}(x,y;\varepsilon_0)=\frac{1}{T}\int_t^{t+T}V(x-X(\tau),y)d\tau, \tag{2}$$

where $T=2\pi/\omega$. The analytical form of the above KH well is

$$V_{KH}(x,y;\varepsilon_0)=-\frac{V_0}{\pi}\Theta(r^2-y^2)[\arcsin(\alpha_+)-\arcsin(\alpha_-)], \tag{3}$$

where

$$\alpha_\pm=\begin{cases}1, & x<\pm\sqrt{a^2-y^2}\\ 1\pm\dfrac{\omega^2}{\varepsilon_0}(\sqrt{a^2-y^2}\mp x), & 0<x\mp\sqrt{a^2-y^2}<2\\ -1, & x>2\pm\sqrt{a^2-y^2}.\end{cases} \tag{4}$$

The KH potential for $\varepsilon_0=15$ a.u., $\omega=1$ a.u. and for the radial well [Eq. (1) with $a=1$ a.u., $V_0=2$ a.u., a single bound state] and its two eigenstates are shown in Fig. 1.

III. QUANTUM NUMERICAL RESULTS OF *AB INITIO* SIMULATIONS AND CLASSICAL PREDICTIONS

Because we want to include nondipole effects, we write the atom-field interaction in the velocity gauge. The vector potential $\hat{x}A(ky-\omega t)$ is polarized along the x axis and the Hamiltonian reads

$$\hat{H}(\vec{r},t)=\frac{[\hat{p}+\hat{x}A(ky-\omega t)]^2}{2}+V(\vec{r}), \tag{5}$$

where the radial potential is given by Eq. (1).

We have solved this equation both with and without the dipole approximation using *the alternating direction implicit* method [7], which allows one to use tridiagonal sets of equations which can be solved easily and fast. The main difficulty in the two-dimensional calculation is not the number of operations to be performed by a processor but rather a large memory necessary to store the results. The size of the accessible memory sets a limit to the size of the spatial grid used in the calculation. We performed our calculation on the 2048×2048 grid with the step Δx close to 0.1 a.u. The space range is from -100 a.u. to $+100$ a.u. in both directions.

As mentioned above, the particular form of the vector potential is

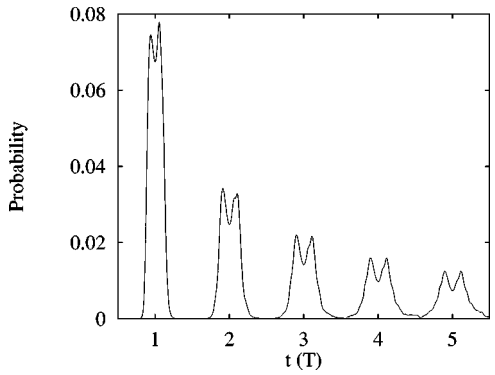

FIG. 2. The population of the initial state. The pulse parameters are $\varepsilon_0=15$ a.u., $\omega=1$ a.u. and the well potential $a=1$ a.u., $V_0=2$ a.u.

$$\vec{A}(y,t)=-\hat{x}\frac{\varepsilon_0}{\omega}\sin(ky-\omega t), \tag{6}$$

with $\omega=1$ a.u. and ε_0 equal to 15 and 20 a.u. Larger values of the vector potential amplitude require a relativistic approach.

At the beginning of each cycle, the left minimum of the KH well occurs close to the packet's initial position in the well; in fact, Eq. (3) yields a shift of the maximum of the wave-packet trapped by the KH well with respect to the initial wave packet's maximum by about 1 a.u. The latter is localized in the KH well's left half and is almost equally divided between the two discrete states. The energy difference between the KH eigenstates is small, so we do not observe any beats, which would occur in a much longer time scale than that considered here. The shift of the minima of the two wells is reflected on the dynamics of the initial-state population (see Fig. 2). The splitting of each peak can be explained by the fact that the maximum of the trapped packet passes by the original well twice at the beginning of each period, with small velocities of opposite signs. This can be treated as an evidence of applicability of KH approach in this range of parameters.

The rest of the initial wave packet, i.e., the part which has not been trapped in the KH well as well as the part initially trapped but later released due to higher terms of the Fourier expansion, is thrown away in the form of concentric rings (see Fig. 3) which oscillate as a whole along the x axis in the rhythm of the field. In the dipole approximation neither turn of the y axis is distinguished but if no dipole approximation is made most of probability will drift towards the positive direction of the y axis due to the magnetic force, according to the classical considerations presented below. The additional structures visible in Fig. 3 will be discussed later.

The vector potential given by Eq. (6) corresponds to the electric and magnetic fields:

$$\vec{E}(y,t)=\hat{x}E(y,t)=\hat{x}\varepsilon_0\cos(ky-\omega t), \tag{7}$$

$$\vec{B}(y,t)=-\hat{z}B(y,t)=-\hat{z}B_0\cos(ky-\omega t), \tag{8}$$

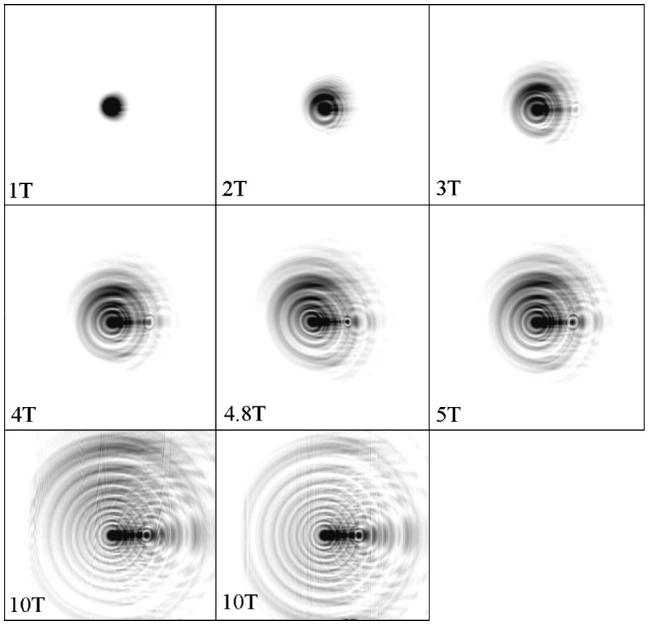

FIG. 3. The modulus square of the wave function after $1T$, $2T$, $3T$, $4T$, $4.8T$, $5T$, $10T$ without the dipole approximation and after $10T$ in the dipole approximation. The distance between the centers in the x direction (horizontal) of the families of the rings is 30 a.u. The atomic and field parameters are the same as in Fig. 2.

where $\vec{k}=\hat{y}k=\hat{y}(y/c)$. Then, the Lorentz force is

$$\vec{F}=-(\vec{E}+\vec{v}\times\vec{B})=-(E-v_yB,v_xB,0). \tag{9}$$

One can write the classical equations of motion for an electron in the electromagnetic field

$$\ddot{x}(t)=-\varepsilon_0\left(1-\frac{\dot{y}(t)}{c}\right)\cos[ky(t)-\omega t],$$

$$\ddot{y}(t)=-\frac{\varepsilon_0}{c}\dot{x}(t)\cos[ky(t)-\omega t], \tag{10}$$

which can be easily solved numerically. The solution of these equations is presented in Fig. 4 (broken line). The upper plot shows fast oscillations with the frequency ω and the same amplitude as for the corresponding one-dimensional solution in the dipole approximation. The lower plot shows the magnetic drift and the oscillations of the frequency 2ω. The velocity of this drift is proportional to the square of electric-field amplitude ε_0. The results can be easily understood if we simplify Eq. (10) neglecting the magnetic component of the Lorentz force in the x direction and neglecting at this stage the y dependence of the field. So we can write the simplified equations of motion

$$\ddot{x}(t)=-\varepsilon_0\cos(\omega t),\ \dot{x}(t)=-\frac{\varepsilon_0}{\omega}\sin(\omega t),$$

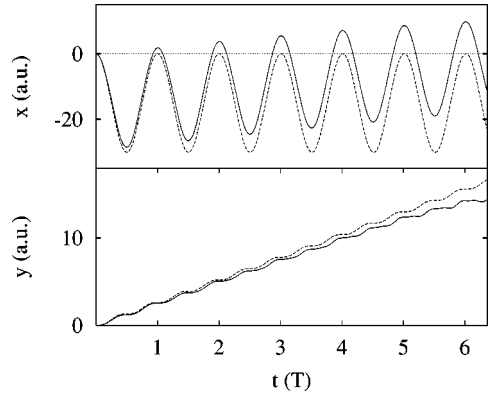

FIG. 4. The mean values of x and y in the quantum simulation, solid lines, compared with the solution of the Newton equations for an unbound electron without the dipole approximation, broken lines. The classical trajectory in the x direction in the dipole approximation coincides with that without this approximation in the scale of the picture. Note the slow drift of the quantum mean value $\langle x\rangle$ imposed on the oscillations of frequency ω and the magnetic drift accompanied by the oscillations of frequency 2ω of both the quantum mean value $\langle y\rangle$ and the classical solution. A cosine pulse is assumed, with the intensity $\varepsilon_0=15$ a.u. and frequency $\omega=1$ a.u.

$$\ddot{y}(t)=-\frac{\varepsilon_0}{c}\dot{x}(t)\cos(\omega t)=\frac{\varepsilon_0^2}{2\omega c}\sin(2\omega t), \qquad (11)$$

with the electron initially resting at $x=y=0$.

This approximation corresponds to the series expansion of vector potential $A_0\sin(ky-\omega t)$ around ωt and leaving only the lowest term [6]. The magnetic drift is directed towards the positive values of y, with oscillations of frequency 2ω imposed on it. The average velocity in the y direction is proportional to the square of the field amplitude.

IV. WAVE-PACKET TEARING AND ITS CONSEQUENCES

The *ab initio* solutions of the Schrödinger equation with Hamiltonian (5) and the laser field defined by Eq. (6) demonstrate that the mean values of the operators x and y look very similar to the free classical predictions (see Fig. 4), as could be expected from the Ehrenfest theorem in the situation in which the electron-laser field interaction dominates the electron-well interaction. We can see fast oscillations of the quantum mean positions in the x direction in the upper plot and the magnetic drift in the y direction in lower one, compared with their classical counterparts. A slow drift, similar to that obtained in Ref. [8], is also visible at the graph of $\langle x\rangle$.

The snapshots of the wave function shown in Figs. 3, 5, and 6 have been taken after an integer number of cycles which means that the whole structure is then in right turning point of the oscillatory motion, i.e., the main peak oscillates between $x=-2\epsilon_0/\omega^2$ and $x=0$, while the additional substructures, which are then visible on the right of the main peak and which will discussed below, oscillate between $x=0$ and $x=+2\epsilon_0/\omega^2$ in the same rhythm as the main peak. The wave functions look quite different from those shown in

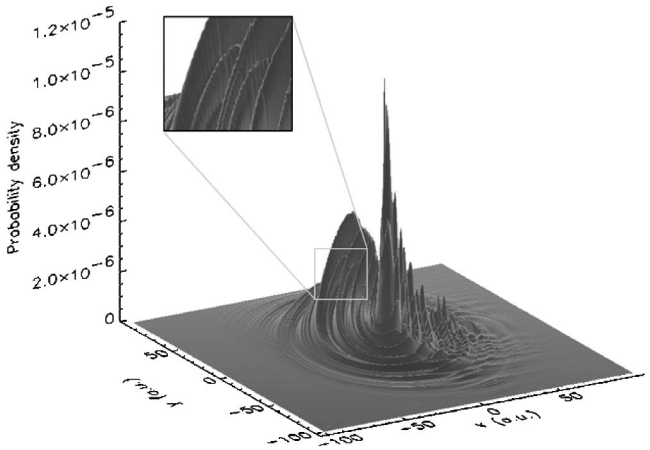

FIG. 5. Modulus square of the wave function after $6T$. One can distinguish fragments thrown away after full cycles from those thrown away in the middle of each cycle (see inset). The parameters of a rectangular cosinusoidal pulse are $\varepsilon_0=20$ a.u., $\omega=1$ a.u. The shift of the probability density towards the region of $y>0$ is well visible.

Refs. [5,6], because here a deep potential well is used instead of a soft-core atom. In spite of the strength of the laser field, the wave function does not behave typically for the over-the-barrier (OTB) ionization regime, in which the packet behaves essentially as a connected structure. Parts of the packet are thrown away in the form of two sets of elliptic rings with centers corresponding to the positions of both minima of the KH well. Those oval structures carry a significant portion of the probability of finding the electron. In the dipole approximation, a new ring appears once a period (Fig. 6). If no dipole approximation is made, the rings appear twice a period with each second ring being due only to the magnetic force oscillating with the doubled frequency [cf. Eq. (11)], this is shown in the inset of Fig. 5. The torn-off structures are thrown preferably towards positive y due to the magnetic interaction. A comparison of the heights of the main peak in Figs. 5 and 6 shows that making the dipole approximation leads to a significant underestimation of the ionization rate.

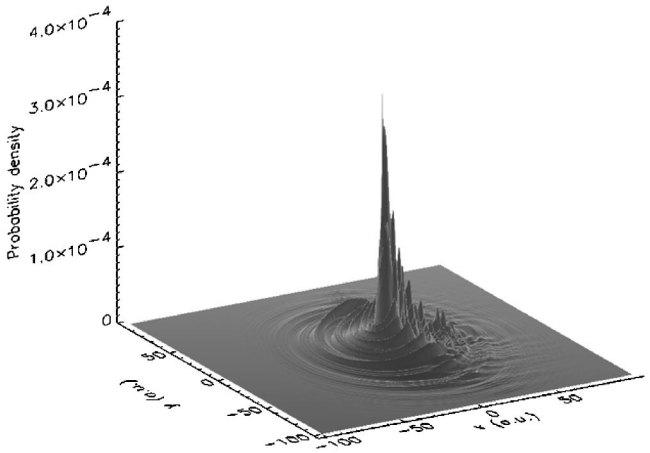

FIG. 6. As in Fig. 5 but in the dipole approximation.

V. RESCATTERING OF THE LIBERATED PARTS OF THE WAVE PACKET

For the cosine rectangular pulse, the wave packet oscillates from 0 to $-2\varepsilon_0/\omega^2$ along the x axis such as in the OTB regime. It is well known that an irreversible ionization of the packet in the form consisting of throwing away pieces of the packet can occur only if both the electric field and the binding potential are present and the packet has a small velocity when passing by the well. Those conditions are satisfied during a significant part of each cycle if the phase of the field is chosen so that the pulse is cosinusoidal. Then, one of the wave packet's turning points is located at the well so once a cycle an electron has the possibility to be liberated. In the case of a sine pulse with a trapezoid envelope (not shown here), there is no opportunity for any packet tearing in such strong laser fields until the wave packet is wide enough to cover the range of classical oscillations (i.e., the width of the KH well). In this case, rings appear a few cycles later then in the case of cosine pulse.

As described above, for a cosine pulse at the end of each cycle, when the packet is stopping above the well, a part of the packet is thrown away from the well and forms a ring around the main part of the packet. Thus, the wave function takes the shape of rings around the main maximum, oscillating as a whole in the x direction. After a few periods the first oval structure reaches a radius of the order of $2\varepsilon_0/\omega^2$, so there is some probability of finding the electron at the well at the moment at which the classical turning point occurs at $-2\varepsilon_0/\omega^2$, i.e., after an odd multiple of half a cycle. Tearing this secondary cloud causes a creation of a second family of rings, which are centered at the distance $2\varepsilon_0/\omega^2$ from the center of the first family of rings and obviously carry a smaller portion of the probability.

The most interesting effect is an interference of both families of the rings giving rise to an additional structure between two turning points and to a complicated shape of the wave function at larger x [see Fig. 3 (the wave function after $10T$ computed in dipole approximation) and Figs. 5 and 6]. This interference effect has no magnetic character and occurs similarly both in the general case and in the dipole approximation.

This new type of rescattering can be even easily understood using the KH model. In the Kramers frame, i.e., in the frame oscillating like an unbound electron, the two wave-packet's turning points correspond to the two turning points of moving potential and, after time averaging, approximately to the minima of the KH well (for cosine pulse: $x=0$ and $x=+2\varepsilon_0/\omega^2$). Because for the field magnitude used in this paper, the KH well has two states with close energies (see Fig. 1), the electron is located in such a superposition of those states that only the left minimum is significantly populated. The higher terms of the Fourier expansion, characterized by large frequencies but rather small amplitudes, cause an ionization of the trapped wave packet in a way typical of the multiphoton regime: fragments of the wave packet are torn off and sent in all directions. It is how the first, main family of the rings in Fig. 3 is formed. The torn-off pieces, being of a considerable size, are scattered on the other minimum of the KH well, which results in a formation of the second family of rings, centered about $2\varepsilon_0/\omega^2$. Both families of the rings can interfere. In particular, this is visible for the parts moving along the x axis: a pattern structure is built after a few cycles between the two minima of the KH well.

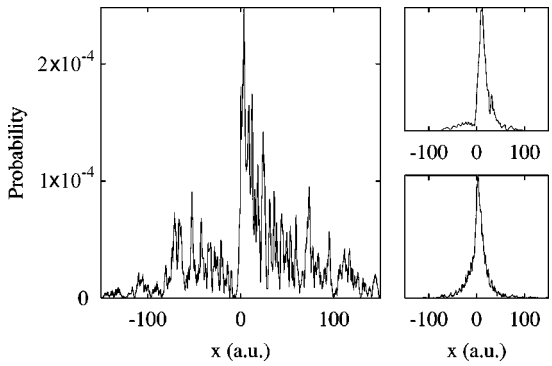

FIG. 7. The main picture: a one-dimensional wave packet for a rectangular pulse with the parameters as in Fig. 3 and the well potential chosen to match the energy of only state $E_1=-0.832$ a.u. The small pictures: upper wave packet, the same field but for a soft-core atom; lower wave packet, the well potential four times less deep than in the main picture (the maxima on the small pictures have the height of about 0.0004 a.u.). All the snapshots were taken after $10T$.

In the case of a sine pulse with a trapezoid envelope, the mechanism of tearing is similar as described above. An important difference is that it takes a few cycles for the packet to become broad enough so that it reaches the minima of the KH well and can be ionized by higher terms of the Fourier expansion. After that period the packet is rescattered on both minima of the KH well, and so both families of rings appear simultaneously.

Our observations in two dimension allowed us to complete the interpretation of the one-dimensional results: a very similar interference structure in the form of numerous subpeaks between the classical turning points can also be seen in the results of one-dimensional computations (see Fig. 7). The effect is significantly reduced if the well is made more shallow or if it is replaced by a soft-core potential.

VI. CONCLUSIONS

We have presented a detailed dynamical picture of two-dimensional photodetachment in very strong fields in the parameters range not explored before. Due to the steep edges of the rapidly varying well potential for some model pulses one can observe tearing smaller pieces off the main packet. The latter pieces can themselves be torn into fragments, giving rise to new spatial structures of the wave packet, possibly interfering with the old ones. We have demonstrated those elements of the dynamics that are due to the binding potential being short range. The behavior of the packet described above is to be contrasted with the packet's dynamics in the case of a smooth binding potential, in which a connected structure is trapped in the KH well and possibly push out by the magnetic force.

[1] M. Gavrila, J. Phys. B **35**, R147 (2002).
[2] For example, J.H. Eberly, R. Grobe, C.K. Law, and Q. Saw, in *Atoms in Intense Laser Fields*, edited by M. Gavrila (Academic Press, Boston, 1992), p. 301.
[3] Ionization in arbitrary polarization, see, e.g., M. Protopapas, D.G. Lappas, and P.L. Knight, Phys. Rev. Lett. **79**, 4550 (1997); the breakdown of the dipole approximation and magnetic drift, J.R. Vazquez de Aldana and L. Roso, Phys. Rev. A **61**, 043403 (2000); H.R. Reiss, *ibid.* **63**, 013409 (2001).
[4] For example, Q. Su and J.H. Eberly, Phys. Rev. A **44**, 5997 (1991).
[5] M.Yu. Ryabikin and A.M. Sergeev, Opt. Express **7**, 417 (2000).
[6] J.R. Vazquez de Aldana, N.J. Kylstra, L. Roso, P.L. Knight, A. Patel, and R.A. Worthington, Phys. Rev. A **64**, 013411 (2001).
[7] W.H. Press, S.A. Teukolsky, W.T. Vetterling, and B.P. Flannery, *Numerical Recipes* (Cambridge University Press, Cambridge, 1992).
[8] J. Matulewski, A. Raczyński, and J. Zaremba, Phys. Rev. A **61**, 043402 (2000).